NOISE ATTENUATION USING ADAPTIVE WAVELET THRESHOLD BASED ON CEEMD INF-X DOMAIN

MIN JI[1], XIANGYUAN ZHAO[2], WEI ZHU[3], YUCHUN YOU[2], JINFENG ZHANG[4], MOHAN SHANG[2], XIAOYA CHUAI[5], YAJUAN XUE[6], CHENHAO LIAN[7] and WEI CHEN[7]

[1] *Key Laboratory of Marine Oil and Gas Reservoirs Production, Sinopec, Beijing, P.R. China.*
[2] *Petroleum Exploration and Production Research Institute, Sinopec, Beijing 102206, P.R. China.*
[3] *Changqing Industrial Group Co., Ltd, Petro China Changqing Oilfield Branch, Xi'an, P.R. China.*
[4] *No.5 Oil Production Plant, Petro China Changqing Oilfield Branch, Xi'an, P.R. China.*
[5] *College of Geophysics, China University of Petroleum-Beijing, Beijing 102249, P.R. China. chuaixiaoya007@126.com*
[6] *School of Communication Engineering, Chengdu University of Information Technology, Sichuan, P.R. China.*
[7] *School of Geophysics and Petroleum Resources, Yangtze University, Hubei, P.R. China. chenwei2014@yangtzeu.edu.cn*

(Received November 8, 2022; accepted February 5, 2023)

ABSTRACT

Ji, M., Zhao, X.Y., Zhu, W., You, Y.C., Zhang, J.F., Shang, M., Chuai, X., Xue, Y., Lian, C.H. and Chen, W., 2023. Noise attenuation using adaptive wavelet threshold based on CEEMD inf-x domain. *Journal of Seismic Exploration*, 32: 131-153.

Noise attenuation plays an important role in seismic signal processing. Complementary Ensemble Empirical Mode Decomposition (CEEMD) is a classic algorithm for signal decomposition and is usually used for denoising. This algorithm is used to attenuate random noise by removing some high-frequency intrinsic mode functions (IMFs), apparently resulting in insufficient noise attenuation and loss of effective signal. Wavelet threshold denoising can be used to attenuate the useless part and enhance the useful part of the signal by selecting the appropriate threshold. Wavelet threshold denoising is often combined with CEEMD in time domain to achieve relatively good effects, but some of signal between seismic traces are fragmented. This paper proposes improved adaptive wavelet threshold denoising based on CEEMD in f-x domain. The new threshold function we proposed is constructed on the basis of the traditional soft and hard threshold functions, which overcomes the constant deviation and avoids the phase step phenomenon. The processing results for simulated and field data show that the proposed method has better attenuation effect on random noise than traditional methods.

KEY WORDS: complementary ensemble empirical mode decomposition, intrinsic mode function (IMF), adaptive wavelet threshold.

0963-0651/23/$5.00

INTRODUCTION

In seismic exploration, the acquisition of seismic data always suffers from a large amount of random noise (Huang et al., 2016; Li et al., 2016). Random noise is a kind of interference wave without certain frequency, especially with a tremendous change in the main frequency range (Lin et al., 2015; Chen et al., 2017). Time-frequency analysis is the main method to analyze and process seismic data with random noise (Liu et al., 2012; Liu and Chen, 2013). The Short-Time Fourier Transform (STFT) is a simple time-frequency analysis method of signal. Window function is used in STFT to analyze the signal in the time domain. However, the time window is fixed so that it is difficult to take into account time and frequency simultaneously (Griffin and Jae, 1984). Continuous Wavelet Transform (CWT) is a linear time-frequency analysis method. Time window is also used in CWT, but it is different from STFT because the window scale of CWT is variable. So the time-frequency resolution of CWT is better than that of STFT (Medl, 1998), but the wavelet basis of CWT is difficult to select. Subsequently, S-transform was proposed on the basis of STFT and CWT to solve the problems of the above two time-frequency analysis methods (Stockwell and Mansinha, 1996). Its time window can vary with frequency and its window width can narrow at high frequencies and widen at low frequencies (Liu and Chen, 2019). Although the size of the window function is variable, the shape of the window function is limited by Heisenbergs uncertainty principle (Liu et al., 2011; Ouadfeul and Aliouane, 2014). The above-mentioned time-frequency analysis methods used to be the mainstream of seismic spectrum analysis, but those methods cannot achieve good results when analyzing nonlinear and non-stationary signals, such as seismic signal (Fomel, 2008).

Empirical Mode Decomposition (EMD) was proposed by Huang et al. (1998). EMD is an adaptive time-frequency analysis method, and decomposes the signal into intrinsic mode functions (IMFs) with frequency from high to low.Because random noise is generally a kind of high-frequency signal, high-frequency IMF1 or IMF1 and IMF2 can be subjectively removed (Chen et al., 2015; Chen and Fomel, 2018). However, modal mixing may occur when using EMD method. Modal mixing means that the waveforms of adjacent IMFs are always mixed, so it is difficult to make effective judgment during denoising (Chen and Ma, 2014). Aiming at the modal mixing phenomenon, Wu et al. proposed the Ensemble Empirical Mode Decomposition (EEMD) (Wu and Huang, 2009). According to the uniform distribution of white noise, EEMD can be used to separate signals with different frequencies, which can solve the problem of mode mixing (Han and Mirko, 2015). EEMD is used to solve the modal mixing phenomenon of EMD effectively, but it causes more errors and increases the amount of calculation due to the addition of a large amount of white noise. CEEMD was proposed in view of the shortcomings of the EMD and EEMD (Chen et al., 2017). CEEMD is characterized by adding positive and negative white noise to the signal, which solves the problems of EMD and CEEMD. The positive and negative white noises can cancel each other out to reduce errors. Experiments show that

CEEMD has better separation effect of modal mixing and the reconstruction of the original signal is more accurate (Colominas et al., 2014; Sun et al., 2020).

The wavelet threshold is a conventional method to attenuate noise (Morlet et al., 1982; Hess and Wickerhauser, 1996; Zhang et al., 2001). Wavelet coefficients of effective signal and noise have different performances. Wavelet threshold method is used to process those wavelet coefficients through a threshold function to obtain new coefficients. Finally, reconstructing those coefficients by inversing wavelet transform to obtain the denoised signal (Zhu et al., 1997; Chakraborty and Okaya, 1995; Zhang and Ulrych, 2003). The selection of threshold and threshold function is the key of the wavelet threshold denoising (Qu et al., 2016). Using global threshold can effectively attenuate noise, but it removes a large number of useful signals (Xu et al., 2011; Wang et al., 2015. The problem with traditional soft threshold function is constant deviation that the reconstructed wavelet coefficients cannot completely represent original signal. The step phenomenon exists in the traditional hard threshold function and causes a big error to the result (Liu et al., 2016). Aiming at the problems of soft and hard threshold function in processing wavelet coefficients, we improved the new threshold function on the basis of the soft threshold function. The new wavelet threshold function overcomes the problems of the traditional threshold function. The processed wavelet coefficients can recover the signal to a greater extent and filter the noise effectively. The effect of wavelet threshold denoising is greatly improved.

In order to achieve better denoising ability of CEEMD, wavelet threshold denoising method based on CEEMD was proposed. In this method, CEEMD is used to decompose the noise signal. The normalized autocorrelation function is used to analyze the autocorrelation coefficient of the noise signal. The IMFs dominated by noise are found through analysis, and then wavelet threshold denoising is performed on these IMFs. All IMFs and residual components are integrated to obtain the denoised seismic signal. It is further demonstrated that this method has better effect in seismic noise attenuation by comparing with several other conventional methods.

Although the adaptive wavelet threshold based on CEEMD can attenuate random noise, some signals between seismic traces are fragmented. We also tested CEEMD in frequency domain, but some effective signals of the in-phase axis with large tilt angle are lost during attenuating random noise. So we propose combining CEEMD with the improved wavelet threshold in f-x domain on the basis of the original algorithm. First, the original signal is divided into real and imaginary parts in the frequency domain, and each part is decomposed by CEEMD separately. Then the wavelet threshold denoising is performed on the IMF dominated by noise. Finally, the real and imaginary parts are combined and the signal is transformed from the frequency domain back to the time domain. Experiments show that denoising effect doesn’t

change with different tilt angles of the in-phase axis. The signal processing between the seismic traces and the resolution of the seismic data are further improved, and the loss of effective signal is reduced. The proposed method is compared with the other methods, which further illustrates the performance of the proposed method in noise attenuation.

COMPLEMENTARY ENSEMBLE EMPIRICAL MODE DECOMPOSITION

The CEEMD is improved on the basis of EMD and EEMD. EEMD and CEEMD were proposed to solve the problem of modal mixing in EMD. These two methods are used to change the distribution of extreme points by noise assistance. CEEMD retains the completeness of the EMD algorithm, and effectively alleviates the error in EEMD caused by adding a lot of white noises. Using CEEMD can relatively save computing time and ensure the accuracy of each IMF, which benefits to the subsequent signal reconstruction. The steps for CEEMD decomposition are as follows:

1) by adding positive and negative pairs of N groups Gaussian white noises n_i^1(t) and n_i^2(t) to the original seismic signal s(t), 2N signals $n_{i,1}$(t) and $n_{i,2}$(t) containing positive and negative white noises are obtained:

$$n_{i,1}(t) = s(t) + n_i^1(t) \quad , \tag{1}$$

$$n_{i,2}(t) = s(t) + n_i^2(t) \quad . \tag{2}$$

2) perform EMD decomposition on signal $n_{i,1}$(t) and signal $n_{i,2}$(t) to obtain two sets of IMFs and the remaining components r_1^i and r_2^i, then:

$$\mathrm{n}_{i,1}(t) = \sum_{j=1}^{N} imf_{1,j}^i + r_1^i \quad , \tag{3}$$

$$\mathrm{n}_{i,2}(t) = \sum_{j=1}^{N} imf_{2,j}^i + r_2^i \quad . \tag{4}$$

3) the two sets of IMFs are accumulated and averaged to obtain the corresponding IMFs, then the j-th IMF and the remaining component of the original signal can be expressed as

$$\mathrm{imf}_j = \frac{1}{2N} \sum_{i=1}^{N} (imf_{1,j}^i + imf_{2,j}^i) \tag{5}$$

$$\mathrm{R} = \frac{1}{2N} \sum_{i=1}^{N} (r_1^i + r_2^i) \tag{6}$$

The high-frequency IMF1 or IMF1 and IMF2 are generally discarded in the CEEMD method, and the other IMFs and the remaining component are accumulated to obtain the denoised signal.

WAVELET THRESHOLDING DENOISING

Basic principles

Wavelet transform is a linear transform method that analyzes the signal segmentally by adding a variable time window. Wave transform is often used in signal processing and has the characteristics of multi-scale, low entropy and de-correlation. The wavelet threshold denoising is an application of wavelet transform. The basic principles of traditional wavelet threshold denoising are as follows:

1) A set of wavelet decomposition coefficients $\omega_{g,k}$ is obtained by applying wavelet transform to the original signal s(t).

$$\omega_{g,k} = W(s(t)) \quad , \tag{7}$$

where $W(\cdot)$ is the wavelet transform; g is the decomposition level; k is the parameter of translation operation in wavelet transform.

2) A set appropriate threshold and threshold function. If $\omega_{g,k} < \lambda$, then the coefficient is the high-frequency noise coefficient, and the coefficient is directly removed; if $\omega_{g,k} \geq \lambda$, the coefficient is the low-frequency effective signal coefficient, and the coefficient needs to be retained. The traditional soft and hard threshold functions are shown in formulas (8) and (9):

$$\widehat{\omega_{g,k}} = \begin{cases} sgn(\omega_{g,k})(|\omega_{g,k}| - \lambda), & |\omega_{g,k}| \geq \lambda \\ 0, & |\omega_{g,k}| < \lambda \end{cases} \quad , \tag{8}$$

$$\widehat{\omega_{g,k}} = \begin{cases} \omega_{g,k} & |\omega_{g,k}| \geq \lambda \\ ! & |\omega_{g,k}| < \lambda \end{cases} \quad . \tag{9}$$

3) Perform inverse wavelet transform on the processed coefficients to reconstruct the denoised signal.

The key to wavelet threshold denoising is the selection of threshold and threshold function. In wavelet transform, the coefficient corresponding to effective signal is large, while the coefficient corresponding to noise is small. If the selected threshold is too large, the effective signal will be lost. If the threshold is too small, it will cause insufficient denoising. Therefore, whether the appropriate threshold is chosen has a great influence on the denoising effect. Traditional wavelet threshold can be roughly divided into global fixed threshold and local adaptive threshold. Global threshold means that the same threshold is used in wavelet threshold denoising. Local adaptive threshold can generate different thresholds according to different layers

and directions of decomposition. Because the seismic signal is nonlinear and nonstationary, using global fixed threshold may cause the loss of effective signal or the inability to attenuate noise clearly. Therefore, this paper uses adaptive threshold, its expression is as follows:

$$\lambda = \frac{\sigma\sqrt{2\ln(N)}}{g} \quad , \tag{10}$$

where σ is the noise variance, the calculation method is:

$$\sigma = \frac{median(|W_{g,k}|)}{0.6745} \quad . \tag{11}$$

$\omega_{g,k}$ is the wavelet decomposition coefficient; N is the length of each layer of wavelet coefficients; g is the layer number of wavelet decomposition.

In order to solve the constant deviation of soft threshold function and avoid the phase step phenomenon of hard threshold function, this paper constructs a new threshold function. The new threshold function has the following characteristics:

1. the function is continuous at $|\omega_{g,k}| = \lambda$;

2. when $|\omega_{g,k}| \to \infty$, $\widehat{\omega_{g,k}} \to \omega_{g,k}$.

According to the above characteristics, the mathematical expression of the threshold function is:

$$\widehat{\omega_{g,k}} = \begin{cases} \operatorname{sgn}(\omega_{g,k})\left(|\omega_{g,k}| - \dfrac{\lambda}{\exp(\sqrt{\omega_{g,k}^{\,2} - \lambda^2})}\right), & |\omega_{g,k}| \geq \lambda \\ 0, & |\omega_{g,k}| < \lambda \end{cases} \quad . \tag{12}$$

The mathematical analysis of this function is as follows:

a) Continuity of $\widehat{\omega_{g,k}}$: while $\omega_{g,k} \to \lambda^+$, the right limit is $\lim_{\omega_{g,k}\to\lambda^+} \widehat{\omega_{g,k}} = 0$; while $\omega_{g,k} \to \lambda^-$, the left limit is $\lim_{\omega_{g,k}\to\lambda^-} \widehat{\omega_{g,k}} = 0$. So the value of the new threshold function at $\omega_{g,k} = \lambda$ is:

$$\widehat{\omega_{g,k}}(\lambda) = sgn(\lambda)\left(|\lambda| - \frac{\lambda}{exp(\sqrt{\lambda^2 - \lambda^2})}\right) = 0 \quad . \tag{13}$$

It can be seen from the above analysis that $\widehat{\omega_{g,k}}$ is continuous when $\omega_{g,k} \to \lambda$, so as to avoid the phase step phenomenon.

b) Asymptotic property of $\widehat{\omega_{g,k}}$: while $\omega_{g,k} \to \infty$,

$$\lim_{\omega_{g,k}\to\infty}(\widehat{\omega_{g,k}} - \omega_{g,k}) = \lim_{\omega_{g,k}\to\infty}\left[(|\omega_{g,k}| - \frac{\lambda}{\exp(\sqrt{\omega_{g,k}^{\ 2} - \lambda^2})}) - \omega_{g,k}\right] = \lim_{\omega_{g,k}\to\infty}(|\omega_{g,k}| - \omega_{g,k}) = 0 \tag{14}$$

$$\lim_{\omega_{g,k}\to\infty}\frac{\widehat{\omega_{g,k}}}{\omega_{g,k}} = \lim_{\omega_{g,k}\to\infty}\frac{|\omega_{g,k}| - \frac{\lambda}{\exp(\sqrt{\omega_{g,k}^{\ 2} - \lambda^2})}}{\omega_{g,k}} = \lim_{\omega_{g,k}\to\infty}\frac{|\omega_{g,k}| - 0}{\omega_{g,k}} = 1 \tag{15}$$

According to the above derivation, the asymptote of the new threshold function is $\widehat{\omega_{g,k}} = \omega_{g,k}$. The new threshold function solves the problem of constant deviation of the soft threshold function.

Draw the curve of the soft and hard threshold functions and the new threshold function. As shown in Fig. 1, the problems of the traditional threshold functions are solved by the new threshold function.

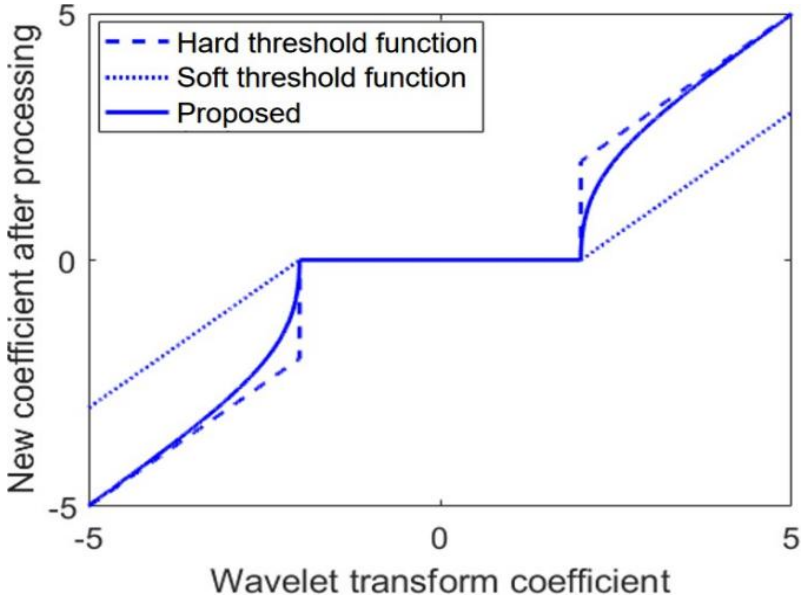

Fig. 1. Traditional threshold functions and new threshold function.

ADAPTIVE WAVELET THRESHOLD DENOISING BASED ON CEEMD

Basic Principles

By analyzing the problems of the traditional methods, adaptive wavelet threshold denoising based on CEEMD is mainly improved from two aspects:

1. One is how to select the IMFs which dominated by noise;
2. The other is to select the threshold and threshold function.

For the first aspect, the theory of normalized autocorrelation function is introduced. The normalized autocorrelation function of the noise-dominated IMF gets the maximum value and appears as a sharp pulse at the zero point. While the value of other points decrease rapidly due to the weak correlation. The the normalized autocorrelation function of IMF dominated by effective signal also has a maximum value at the zero point, but it does not decay rapidly at other points due to the strong correlation between the signals. Fig. 2 is a signal dominated by noise and its normalized autocorrelation function. Fig. 3 is a signal dominated by effective signal and its normalized autocorrelation function. The difference between the two signals can be clearly seen from the two figures.

The second aspect includes the selection of threshold and threshold function. An appropriate threshold can minimize the problems of incomplete denoising or excessive denoising. A suitable threshold function can make the result smoother and clearer. This paper constructs a new threshold function to solve the problems of soft and hard threshold functions. Compared with traditional soft and hard threshold functions, using the new threshold function will not lead to phase step phenomenon and constant deviation problem.

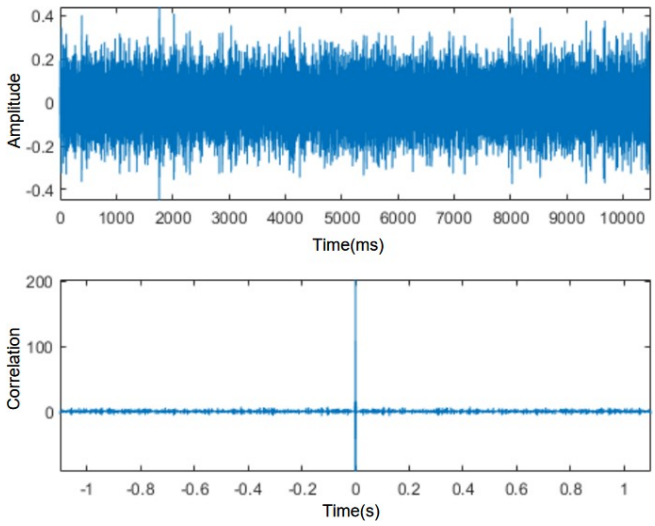

Fig. 2. Signal dominated by noise and its normalized autocorrelation function curve.

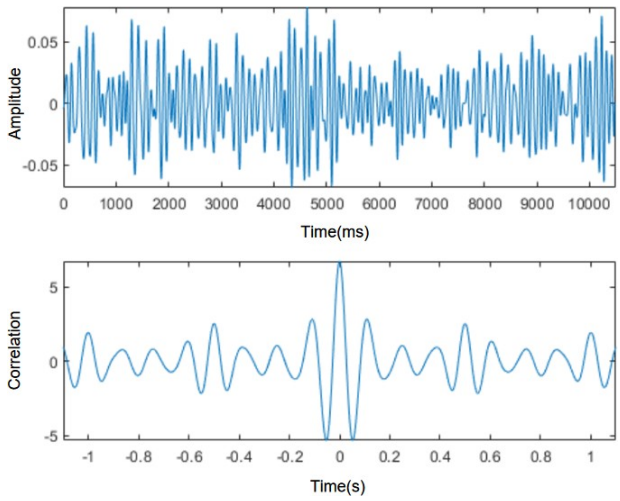

Fig. 3. Signal dominated by effective signal and its normalized autocorrelation function curve.

According to the characteristics of the normalized autocorrelation function of the above two signals. Draw the normalize autocorrelation functions of all IMFs decomposed by CEEMD, and select the IMFs dominated by noise. The processes of adaptive wavelet threshold based on CEEMD are:

1. Decompose the original signal s(t) by CEEMD to obtain the IMFs with frequency from high to low;
2. Draw the normalized autocorrelation function of each IMF and select the IMFs that dominated by noise;
3. Denoising noise-dominated IMFs by adaptive wavelet threshold function;
4. The processed IMFs, the unprocessed IMFs and the remaining component are reconstructed to obtain the denoised data.

Normalized Autocorrelation Function Analysis

Different dimension units are often used for different evaluation indexes. In order to eliminate the inconvenient influence of different dimensions on analysis, it is necessary to standardize the data. Normalization is to transform the data into a fixed interval range which is usually 0 to 1. The differences and influences caused by different sample data can be eliminated by normalization. The following formula is for normalizing the signal, x_{norm} is the normalized result, x is the original data set, x_{max} and x_{min} are the maximum and minimum values in the signal respectively.

$$x_{norm} = \frac{x - x_{min}}{x_{max} - x_{min}} \quad . \tag{16}$$

The autocorrelation function is used to analyze the correlation of each data point of the signal. It also can be used to show the correlation of each value of a signal at different times, especially the correlation of some random sequences. The autocorrelation function of the signal at two different moments can be calculated from the following equation:

$$R_{\mathrm{x}}(\tau) = \lim_{\mathrm{T}\to\infty} \frac{1}{\mathrm{T}} \int_0^{\mathrm{T}} \mathrm{x(t)x(t+\tau)dt} \quad ,$$

R represents the correlation between two points, $x(t)$ is the signal to be analyzed, and τ is the interval between two time points of one signal.

f-x CEEMD

Basic principles

Compared with the effective seismic signal, the random noise has higher frequency and faster vibration. It is more intuitive and convenient to process the signal directly in the frequency domain. According to the frequency characteristics of random noise and effective signal, the IMFs are screened in f-x domain to achieve more accurate denoising effect. The steps of f-x CEEMD are as follows:

1. Transform the noisy seismic signal from time domain to frequency domain by Fourier transform;
2. Separating the real and imaginary parts of the data in the frequency domain;
3. The real part of the signal was decomposed by CEEMD to obtain a series of IMFs corresponding to real part. The noise-dominated IMFs were removed to obtain denoised data in real part;
4. Perform the same operation as in eq. (3) on the imaginary part of the signal;
5. Add the real and imaginary parts of denoised data to obtain the denoised data in frequency domain;
6. Transform data from frequency domain back to time domain;
7. Continue to do the same operation as above for the next time window until the operation of all window functions is completed.

Comparison of Denoising for Different Construction Types and Tendencies

The denoising ability of the proposed method is tested by using simulated data. The simulated data includes in-phase axis, intersections, breakpoints and faults. 50% white Gaussian noise was added to the simulated data, and the experimental results are shown in Fig. 4. Using f-x CEEMD can effectively attenuate the random noise of horizontal in-phase axis, breakpoint and fault structure, and almost does not affect the continuity and resolution of in-phase axis. As shown in Fig. 4(c), the in-phase axis with small tilt angle is well preserved and the noise attenuation effect is significant. While the in-phase axis with large tilt angle is removed together with random noise. As shown by the four red arrows in Fig. 4, the inclined in-phase axis is attenuated by f-x CEEMD, but the data at the intersection point of the horizontal and inclined in-phase axis are not affected. It indicates that this method will not lose the information at the intersection point while attenuating the inclined in-phase axis with large inclination. It has a good protective effect on the effective signals except the inclined in-phase axis.

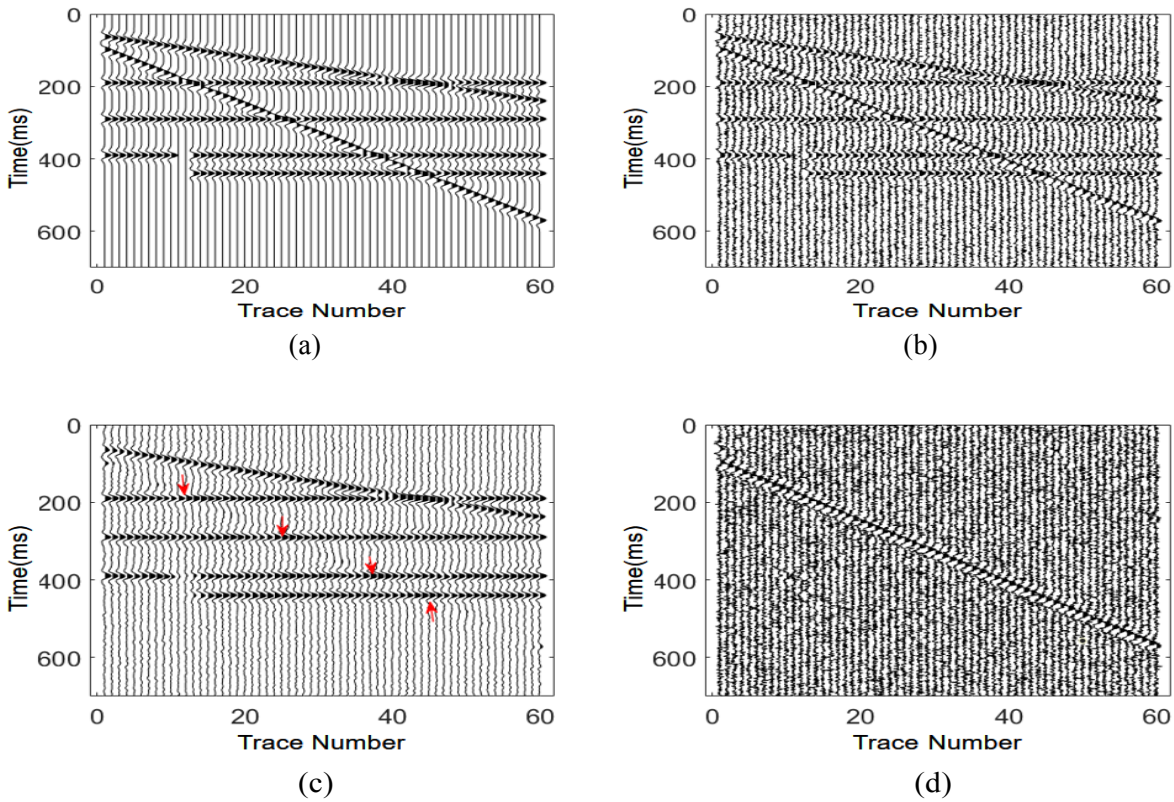

Fig. 4. Simulation data denoising effect: (a) Clean data. (b) Noisy data. (c) Denoising by f-x CEEMD. (d) Denoising residuals.

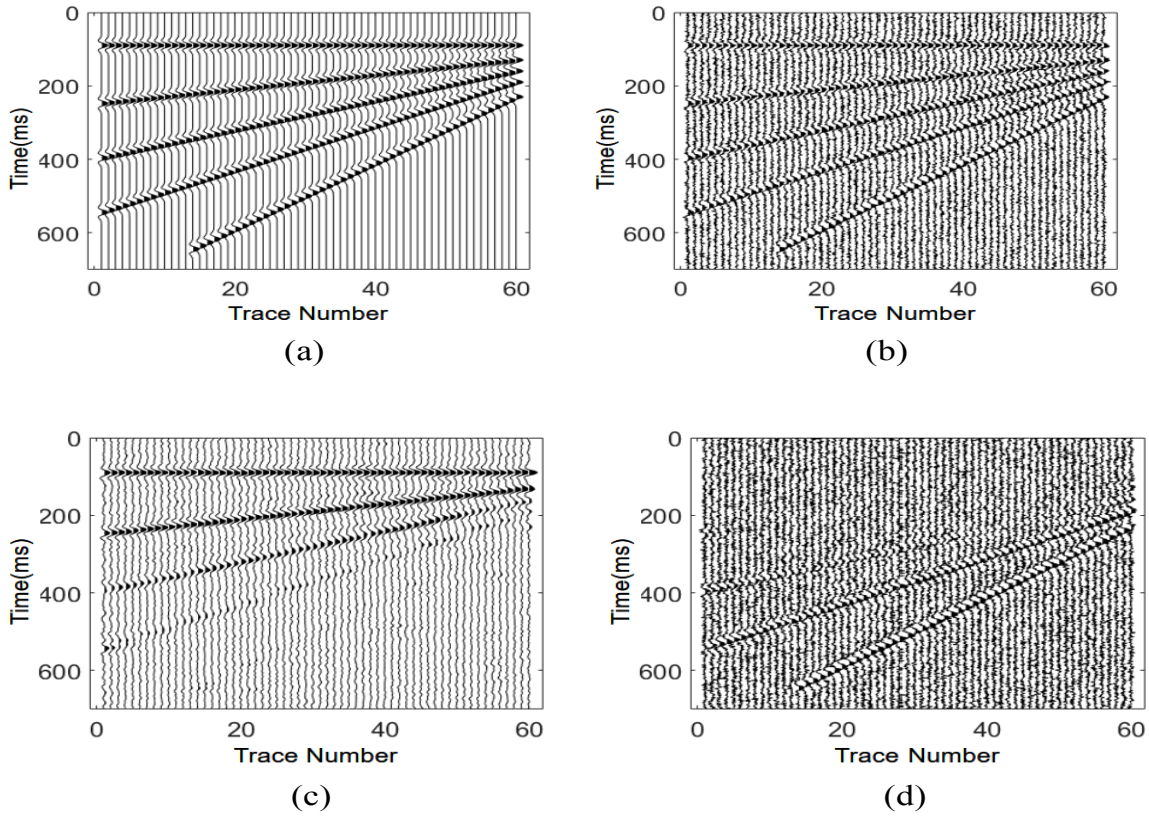

Fig. 5. Simulation data denoising effect: (a) Clean data. (b) Noise data. (c) Denoised using f-x CEEMD. (d)Denoising residuals.

Other simulated experiments are carried out to verify the results. The same Ricker wavelet and seismic reflection coefficients are used to simulate the inclined in-phase axis with different tilt angles. The simulated data contains five inclined in-phase axis, and the tilt angles of the inclined in-phase axis increase successively from top to bottom. 50% Gaussian random white noise was added in the simulated data. And f-x CEEMD was used to attenuate the random noise of the simulated data with different tilt angles. The processed results and residuals are shown in Figs. 5(c) and 5(d). It can be seen that the denoising effect of f-x CEEMD is very different for the in-phase axis with different tilt angles. Although the random noise is almost completely removed, the loss of effective signal is more serious for the in-phase axis with larger tilt angle.

In the above analysis, the loss of the in-phase axis with large tilt angle is serious when using f-x CEEMD. Is this situation related to the tilt direction of in-phase axis? To solve this problem, figure 6 shows five inclined in-phase axis with the same tilt angle and different tilt directions as shown in Fig. 5. 50% white Gaussian noise is also added to the simulated data. The denoising results obtained by using the f-x CEEMD are shown in Figs. 6(c) and 6(d). The in-phase axis with a large tilt angle still has a serious loss even if the tilt direction of the in-phase axis is changed. It is further shown that CEEMD produces

different denoising effects because of the different tilt angle of the in-phase axis. This denoising characteristic has nothing to do with the noise intensity, structure type and tilt direction of the in-phase axis, but only with the tilt angle of the in-phase axis. The larger the tilt angle, the more effective signals of the in-phase axis are attenuated.

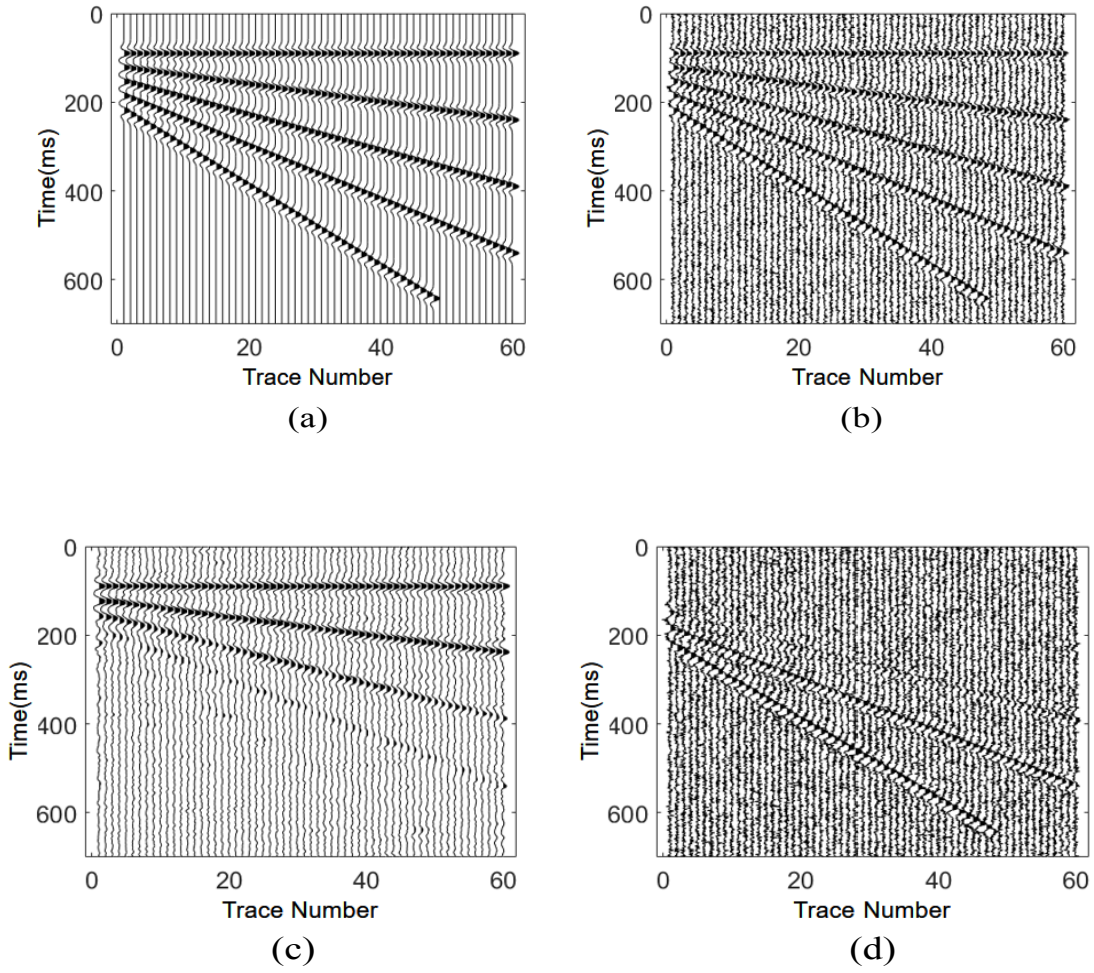

Fig. 6. Simulation data denoising effect: (a) Clean data. (b) Noise data. (c) f-x CEEMD. (d) Denoising residuals.

ADAPTIVE WAVELET THRESHOLD DENOISING BASED ON CEEMD IN F-X DOMAIN

When CEEMD and adaptive wavelet threshold are combined in f-x domain, the original signal is firstly divided into real part and imaginary part in frequency domain. Each part is decomposed by CEEMD, and then the noise-dominated IMFs are denoised by wavelet threshold. Finally, the real and imaginary parts are merged to transform the signal from frequency domain back to time domain. This section is mainly to further explore the denoising effect of the new threshold function combined with CEEMD in f-x domain. Similar to wavelet threshold based on CEEMD in time domain, autocorrelation

function analysis and wavelet threshold denoising are also added after CEEMD decomposition. The specific denoising steps are as follows:

(i) Transform the signal from the time domain to the frequency domain using the Fourier transform.
(ii) Decompose the signal into real and imaginary parts in the frequency domain, and perform CEEMD decom-position on the real and imaginary parts respectively;
(iii) Perform normalized autocorrelation analysis function on the decomposed IMFs to find out the IMFs domi-nated by noise;
(iv) Perform wavelet threshold denoising on the noise-dominated IMFs ;
(v) Reconstruct all processed and unprocessed IMFs in the real and imaginary parts of the signal;
(vi) Add the real part and the imaginary part to obtain the denoised data in the frequency domain;
(vii) Transform the data from the frequency domain back to the time domain using the inverse of the Fourier transform.

NUMERICAL SIMULATION EXPERIMENT

The proposed method is tested using the simulated data in Fig. 7. The simulated data in this section have one more anticline structure than the simulated data in Fig. 4. The angle of each point on the in-phase axis of anticline structure is different. Add 50% white Gaussian noise to the clean data, and the Signal-to-Noise Ratio (SNR) of the data is 3.5403dB. The mathematical expression of SNR is:

$$\mathrm{SNR} = 10\lg\left(\frac{P_S}{P_N}\right) \quad , \tag{18}$$

P_S is the effective power of the signal, P_N is the effective power of the noise.

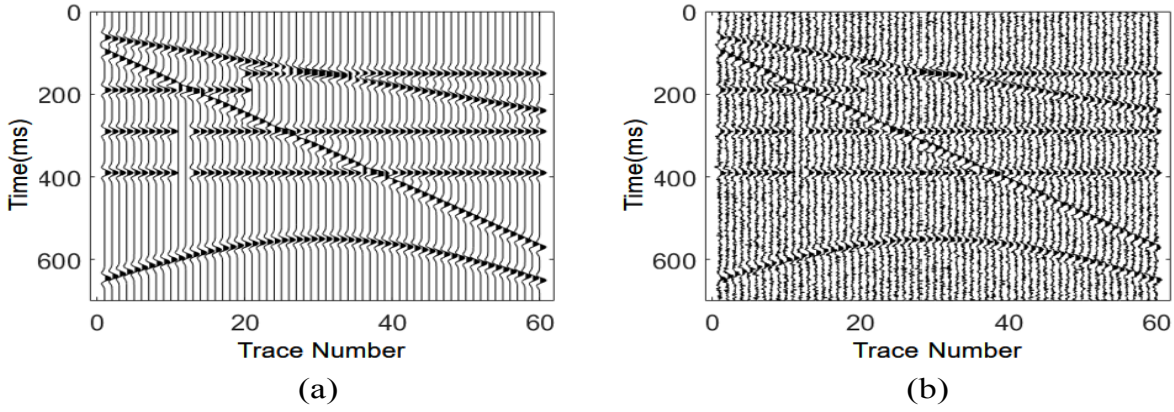

Fig. 7. Synthetic data: (a) Clean data, (b) Noisy data.

The proposed method is compared with the other two methods. The experimental results are shown in Fig. 8. Using the proposed method and f-x CEEMD can effectively attenuate the random noise in the simulated seismic data, and achieve good denoising effects. Although f-x CEEMD can be used to attenuate the random noise in the seismic data well, it obviously attenuates the effective signal of the inclined in-phase axis.

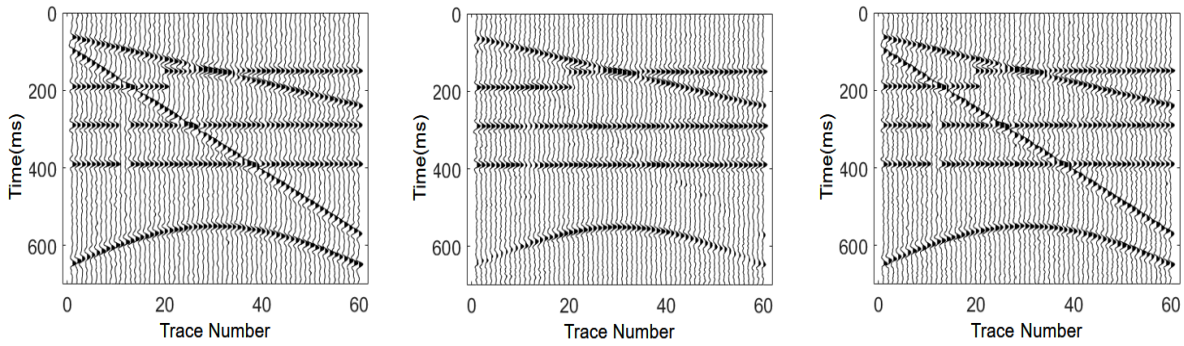

(a) (b) (c)

Fig. 8. Denoising of synthetic data: (a) improved wavelet threshold based on CEEMD, (b) f-x CEEMD, (c) the proposed method.

Fig. 9 shows the denoising residuals of the simulated seismic data by three methods. Wavelet threshold based on CEEMD, f-x CEEMD and the proposed method have good attenuation effect on random noise. By calculating the SNR, the three methods increase the SNR of the simulated seismic data from 3.5403 dB to 9.3235 dB, 7.0631 dB, and 9.9731 dB, respectively. The method in this paper significantly improves the SNR of simulated data. Although the three methods can be used to remove random noise effectively, the inclined in-phase axis with large tilt angle are attenuated when using f-x CEEMD. The loss of effective signal is obvious in the large tilt at both ends of anticline. In contrast, using the proposed method does not lose the inclined in-phase axis with a large tilt angle like f-x CEEMD, and has a better ability to protect the effective signal.

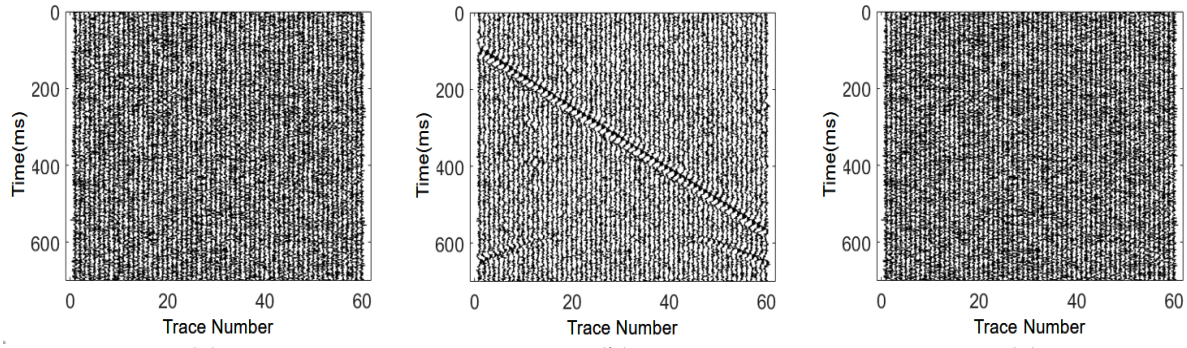

Fig. 9. Denoising residuals: (a) Improved wavelet threshold based on CEEMD, (b) f-x CEEMD, (c) Proposed method.

Fig. 10 shows the F-K spectrum of the clean simulated data and the simulated data adding 50% Gaussian white noise. The energy of the added white noise is evenly distributed in the frequency range. Fig. 11 shows the F-K spectrum of the simulated data after denoising by the three methods. It can be seen intuitively that the seismic data denoised by f-x CEEMD obviously lacks the energy of the inclined in-phase axis with large wave number. And the other two methods can effectively attenuate noise without causing loss of effective signal energy.

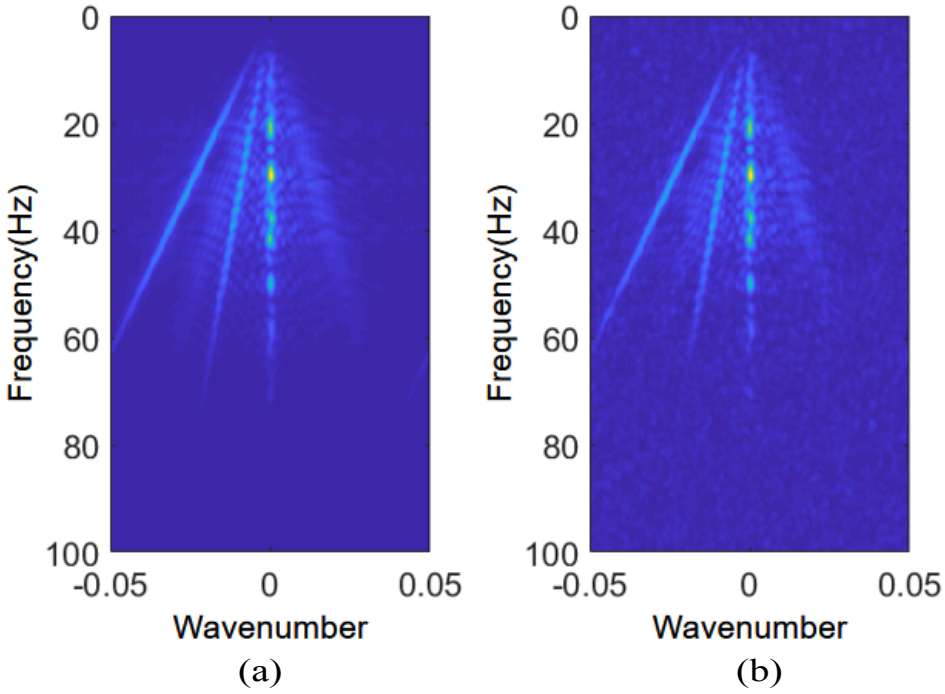

Fig. 10. The F-K spectrum. (a) Clean data. (b) Noisy data.

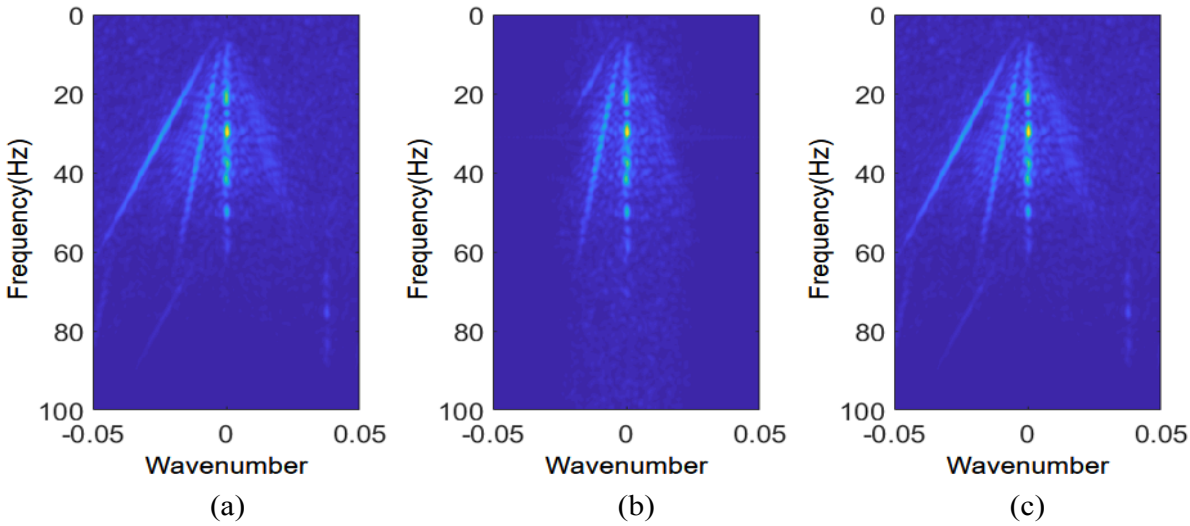

Fig. 11. The F-K spectrums after denoising by three methods: (a) Improved wavelet threshold based onCEEMD. (b) f-x CEEMD. (c) Proposed method.

Fig. 12 shows the comparison of the amplitude spectrum of clean data, noisy data, and the data after denoising by three methods. It can be seen from the figure that the added noise is mainly concentrated at 50-150 Hz. Comparing the two figures, the amplitude of the simulated data denoised by f-x CEEMD is significantly reduced. It confirms the above conclusion once again that f-x CEEMD will cause the loss of effective signals. The other two methods can effectively remove high-frequency random noise, and the amplitude of the effective signal distributed within 0-50 Hz has almost no change. These two methods can protect the effective signal well and reduce the interference of random noise greatly.

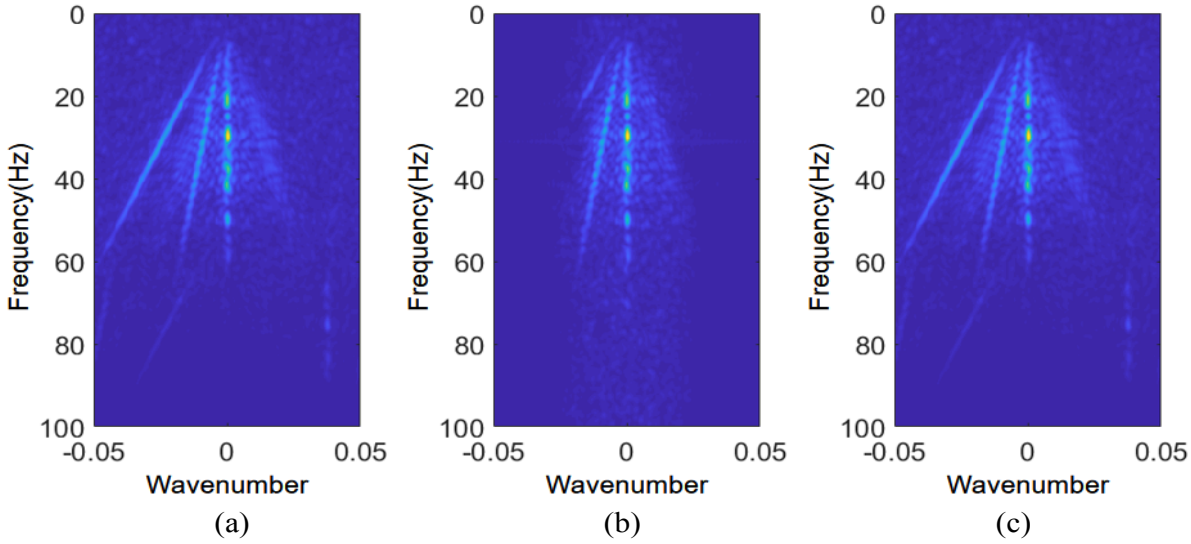

Fig. 12. Amplitude spectrum comparison: (a) Clean data and noisy data. (b) Noisy data denoised using the three methods. (c) Proposed method.

Fig. 13 shows the SNR of simulated data with different noise intensity after denoising by the three methods. According to the figure, SNR is relatively low when using f-x CEEMD due to the loss of effective signals. When the other two methods are used for denoising, the simulated data with different noise intensity can maintain a high SNR. The three methods can maintain the denoising performance when denoising the simulated data with different noise intensity.

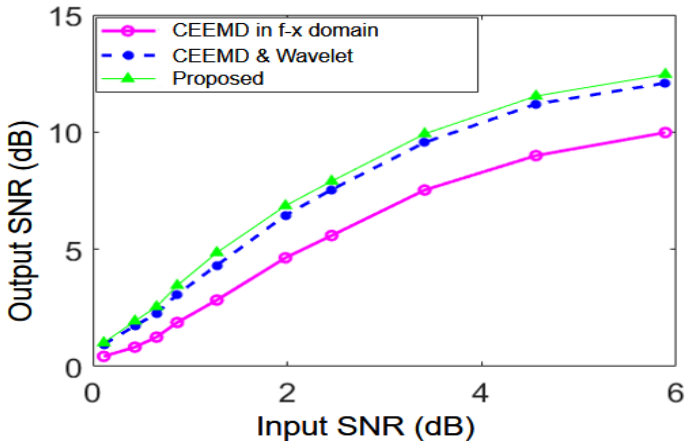

Fig. 13. Three methods denoised SNR at different noise strengths.

REAL SEISMIC DATA TEST

The experimental results of the simulated data show that the wavelet threshold based on CEEMD in time-spaece domain and in f-x domain have good ability in noise attenuation and protection of effective signal. The actual seismic data is shown in Fig. 14. The data contains a total of 201 traces, each trace has 1001 sampling points, and the sampling interval is 1 ms. It can be seen that the actual seismic data contains inclined in-phase axis, curved in-phase axis, faults and breakpoints. However, the actual data is seriously polluted by random noise, and the continuity and resolution of the in-phase axis are very low.

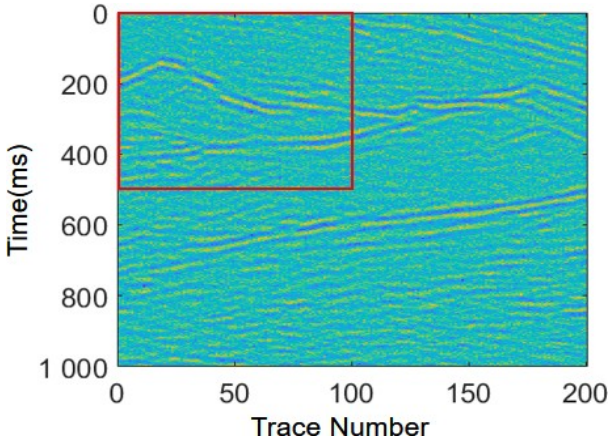

Fig. 14. Field data.

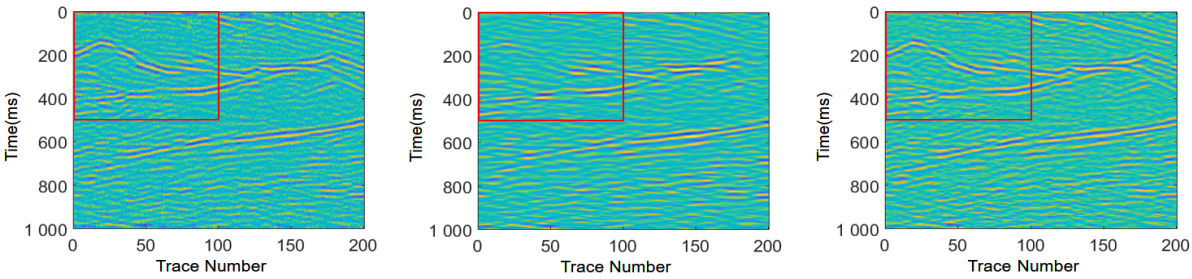

Fig. 15. Denoising of field data: (a) Improved wavelet threshold based on CEEMD, (b) f-x CEEMD, (c)Proposed method.

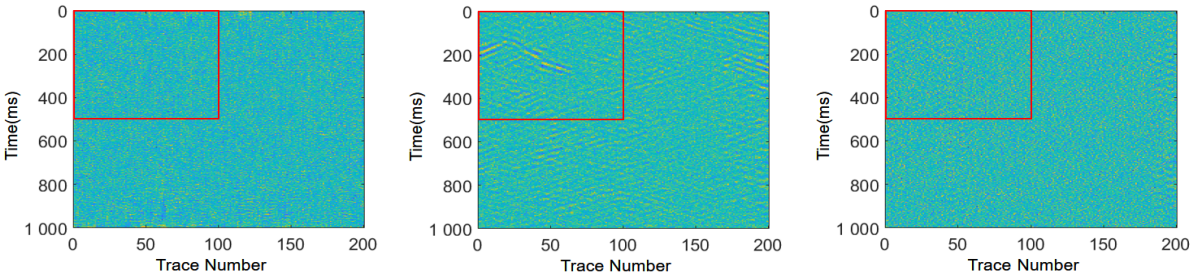

Fig. 16. Denoising residuals: (a) Improved wavelet threshold based on CEEMD. (b) f-x CEEMD. (c) Proposed method.

The actual seismic data after denoising is shown in Fig. 15. The resolution of the seismic data has been significantly improved after denoising by three methods. However, the actual seismic data denoised by f-x CEEMD lacks a lot of effective signals. And the residual signal in Fig. 16 can show that f-x CEEMD removes random noise and also causes the absence of in-phase axis with tilt angle. Comparing the signals in the denoising residuals of the actual seismic data, most of these signals are in-phase axis with large tilt angles. In terms of denoising effect, the resolution of seismic data after denoising by the proposed method is relatively higher. The proposed method runs directly in the frequency domain, which can take into account more details to achieve better denoising effect. Although the adaptive wavelet threshold based on CEEMD can be used to attenuate random noise, some signals between the seismic traces are fragmented.

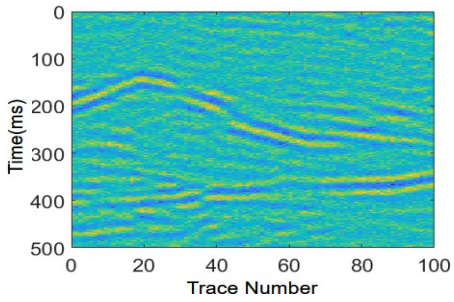

Fig. 17. Part of the field data.

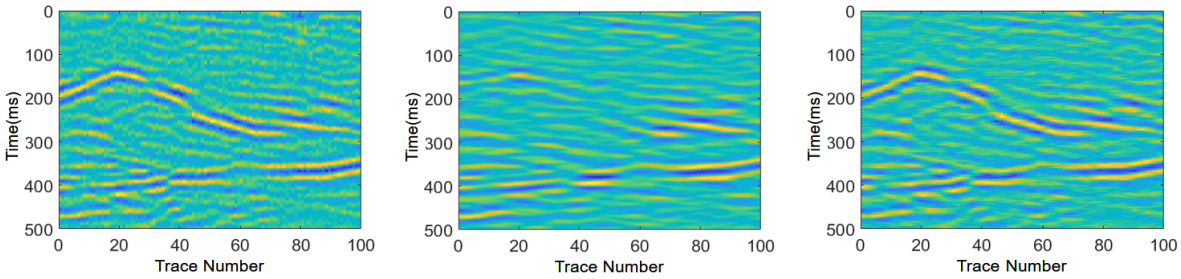

Fig. 18. Denoising of part of field data: (a) Improved wavelet threshold based on CEEMD. (b) CEEMD in f-xdomain. (c) Proposed method.

In order to deeply compare the denoising effect of the three methods as much as possible, we intercept a local real seismic area from 0 ms to 500 ms, 0-th trace to 100-th trace. Each trace includes 500 sampling points and the sampling interval is 1 ms, as shown in Fig. 17. The seismic data processed by wavelet threshold based on CEEMD still contain obvious noise, and the continuity of the seismic tectonic axis is not strong. The proposed method and f-x CEEMD have relatively better denoising effects from Fig. 18. Comparing the denoising residuals for the three methods in Fig. 19, a lot of effective signals with tilt angle were removed when using f-x CEEMD.

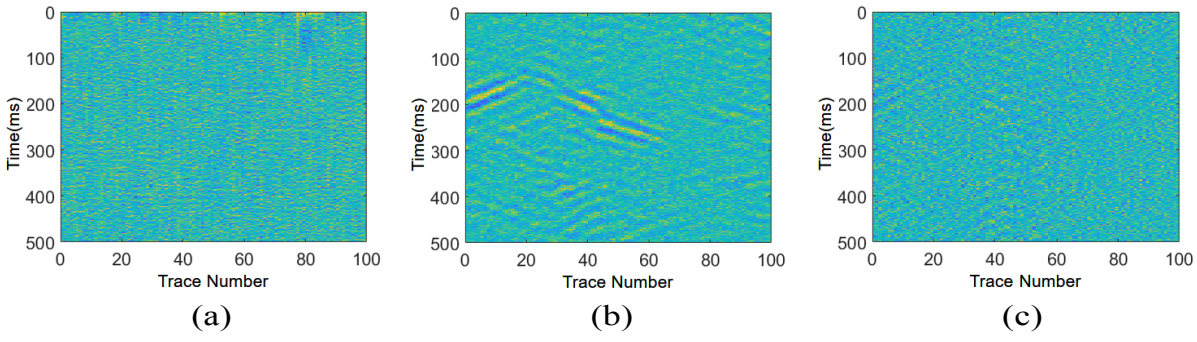

Fig. 19. Removed noise: (a) Improved wavelet threshold based on CEEMD. (b) CEEMD in f-x domain. (c) Proposed method.

DISCUSSIONS

This paper mainly analyzes the ability of three methods to attenuate the random noise. Experiments show that adaptive wavelet threshold based on CEEMD can be used to attenuate random noise, but some signals between seismic traces are fragmented. And f-x CEEMD has a good noise attenuation effect on most of seismic structures, but some effective signals of the in-phase axis with large tilt angle will be lost during attenuating random noise. The larger the tilt angle, the more serious the effective signal loss. In the denoising experiment, the seismic structure type, noise intensity and inclination of the tilt angle are taken as variables. And the multi-directional verification and comparison of the algorithm are carried out. The experimental result shows that the denoising effect of f-x CEEMD has nothing to do with the above variables, but only depends on the magnitude of the tilt angle.

Then, a feasible solution is proposed for the problems existing in f-x CEEMD. CEEMD and wavelet threshold method are combined in f-x domain to attenuate random noise. The denoising results, denoising residuals, F-K spectrum and amplitude spectrum of denoised data show that the proposed method can solve the problem of f-x CEEMD. The proposed method can also be used to attenuate random noise and protect effective signal well. The continuity and resolution of the in-phase axis in the denoised data are improved very well, and the SNR is also greatly improved. Finally, actual seismic data are used to further prove that the proposed method improves the quality of seismic data and provides high-quality seismic data for subsequent seismic data interpretation. It has very important practical significance.

CONCLUSION

We proposed a method in f-x domain for attenuating random noise of seismic data. First, the original signal is divided into real part and imaginary part in the frequency domain, and each part is decomposed by CEEMD. Then, the noise-dominated IMF is denoised by wavelet threshold. Finally, the real part and imaginary part are merged, and the signal is transformed from the frequency domain back to the time domain. This method has a good denoising effect in both simulated data and field data. It not only improve the SNR, but also protect the effective signal and prevent the energy divergence. The proposed method has a better noise attenuation effect by comparing with the traditional methods.

ACKNOWLEDGEMENT

This work was supported in part by the Open Fund of Key Laboratory of Marine Oil & Gas Reservoirs Production, Sinopec, under Grant 33550000-22-ZC0613-0012 and in part by the Natural Science Foundation of Sichuan under Grant 2023NSFSC0258.

REFERENCES

Chakraborty, A. and Okaya, D., 1995. Frequency time decomposition of seismic data using wavelet based methods. Geophysics, 60(6): 1906-1916.

Chen, Y. and Ma, J., 2014. Random noise attenuation by f-x empirical mode decomposition predictive filtering. Geophysics, 79(3): V81-V91, 2014.

Chen, Y., Zhang, G., Gan, S. and Zhang, C., 2015. Enhancing seismic reflections using empirical mode decomposition in the flattened domain. J. Appl. Geophys., 119: 99-105.

Chen, W., Chen, Y. and Cheng, Z., 2017. Seismic time-frequency analysis using an improved empirical mode decomposition algorithm. J. Seismic Explor., 26: 367-380.

Chen, W., Xie, J., Zu, S., Gan, S. and Chen, Y., 2017. Multiple reflection noise attenuation using adaptive randomized order empirical mode decomposition. IEEE Geosci. Remote Sens. Lett., 14: 18-22.

Chen, Y. and Fomel, S., 2018. Emd-seislet transform. Geophysics, 83(1): A27-A32.

Colominas, M., Schlotthauer, G. and Torres, M., 2014. Improved complete ensemble emd: A suitable tool for biomedical signal processing, Biomed. Signal Process. Contr., 14(11): 19-29.

Fomel, S., 2008. Adaptive multiple subtraction using regularized nonstationary regression. Geophysics, 74(1): V25-V33.

Griffin, D. and Jae, L., 1984. Signal estimation from modified short time Fourier transform. IEEE Transact. Acoust., Speech Sign. Process., 32: 236-243.

Han, J. and Mirko, V., 2015. Microseismic and seismic denoising via ensemble empirical mode decomposition and adaptive thresholding, Geophysics, 80(6): KS69-KS80.

Hess, N. and Wickerhauser, M.,1996. Wavelets and time-frequency analysis. Proc. IEEE, 84(4): 523-540.

Huang, N., Shen, Z., Long, S., Wu, M., Shi, H., Zheng, Q., Yen, N., Tung, C. and Liu, H., 1998. The empirical mode decomposition and the Hilbert spectrum for nonlinear and nonstationary time series analysis. Proc. Mathemat. Physic. Engineer. Conf., 454: 903-995.

Huang, W., Wang, R., Chen, Y., Li, H. and Gan, S., 2016. Damped multichannel singular spectrum analysis for 3D random noise attenuation, Geophysics, 81(4): V261-V270.

Li, H., Wang, R., Cao, S., Chen, Y. and Huang, W., 2016. A method for low-frequency noise suppression based on mathematical morphology in microseismic monitoring. Geophysics, 81(3): V159-V167.

Lin, H., Li, Y., Ma, H., Yang, B. and Dai, J., 2015. Matching pursuit based spatial trace time frequency peak filtering for seismic random noise attenuation. IEEE Geosci. Remote Sens. Lett., 12: 394-398.

Liu, G., Fomel, S. and Chen, X., 2011. Time frequency analysis of seismic data using local attributes. Geophysics, 76(6): 23P.

Liu, G., Chen, X., Du, J. and Wu, K., 2012. Random noise attenuation using f-x regularized nonstationary autoregression,Geophysics, 77(2): V61-V69.

Liu, G. and Chen, X., 2013. Noncausal f-x-y regularized nonstationary prediction filtering for random noise attenuation on 3D seismic data. J. Appl. Geophys., 93: 60-66.

Liu, W., Cao, S. and Chen, Y., 2016. Seismic time frequency analysis via empirical wavelet transform. IEEE Geosci. Remote Sens. Lett., 13: 28-32.

Liu, W. and Chen, W., 2019. Recent advancements in empirical wavelet transform and its applications, IEEE Access, 7: 1.

Medl, A., 1998. Time frequency and wavelets in biomedical signal processing. IEEE Engineer. Medic. Biol. Mag., 17 (6): 15-97.

Morlet, J., Arens, G., Fourgeau, E. and Giard, D., 1982. Wave propagation and sampling theory part ii: Sampling theory and complex waves. Geophysics, 47: 222-236.

Ouadfeul, S. and Aliouane, L., 2014. Random seismic noise attenuation data using the discrete and the continuous wavelet transforms. Arab. J. Geosci., 7, 2531-2537.

Qu, S., Zhou, H., Liu, R., Chen, Y., Zu, S., Yu, S., Yuan, J. and Yang, Y., 2016. Deblending of simultaneous source seismic data using fast iterative shrinkage thresholding algorithm with firm thresholding, Acta Geophys., 64:1064-1092.

Stockwell, R. and Mansinha, L., 1996. Localisation of the complex spectrum: The S-transform. IEEE Transact. Sign. Process., 44(4): 998-1001.

Sun, M., Li, Z., Li, Q. and Wang, W., 2020. A noise attenuation method for weak seismic signals based on compressed sensing and ceemd. IEEE Access, 8(99): 1.

Wang, B., Wu, R., Chen, X. and Li, J., 2015. Simultaneous seismic data interpolation and denoising with a new adaptive method based on dreamlet transform. Geophys. J. Internat., 201: 1180-1192.

Wu, Z. and Huang, N., 2009. Ensemble empirical mode decomposition: a noise assisted data analysis method. Advan. Adapt. Data Analys., 1(1): 1-41.

Xu, X., Liu, W., Wang, J., Mu, D. and Qian, Z., 2011. Detection of voltage flicker caused by intergrated wind power based on adaptive lifting wavelet transform, Proced. Engineer., 15: 5105-5110.

Zhang, L., Bao, P. and Pan, Q., 2001. Threshold analysis in wavelet based denoising. Electron. Lett., 37(24): 1485-1486.

Zhang, R. and Ulrych, T., 2003. Physical wavelet frame denoising, Geophysics, 68: 225.

Zhu, X., Shen, Z., Eckermann, S., Bittner, M., Hirota, I. and Yee, J., 1997. Gravity wave characteristics in the middle atmosphere derived from the empirical mode decomposition method. J. Geophys. Res. Atmosph., 102(D14): 16.54-16.561.